International Journal of Automation and Computing 14(4), August 2017, 450-462
DOI: 10.1007/s11633-017-1078-7

Comparative Analysis of Optimized Output Regulation of A SISO Nonlinear System Using Different Sliding Manifolds

M. S. Sunila V. Sankaranarayanan K. Sundareswaran
Department of Electrical and Electronic Engineering, National Institute of Technology, Tiruchirappalli, India

Abstract: This paper presents the design of sliding mode controller for the output regulation of single input single output (SISO) nonlinear systems. The sliding surfaces are designed to force the error dynamics to follow proportional (P), proportional integral (PI) and proportional integral derivative (PID) dynamics. The controller parameters are obtained using probabilistic particle swarm optimization technique. A judicious selection of various sliding surfaces based on the relative degree of the systems is also elaborated. A detailed comparison of the output regulation for various systems with different relative degree is presented. Numerical simulation shows the effectiveness of the proposed method and robustness of the sliding mode controller.

Keywords: Higher order sliding mode, nonlinear system, sliding manifolds, relative degree, probabilistic particle swarm optimization.

1 Introduction

Most of the control systems generally exhibit nonlinear behavior in the presence of uncertainties/disturbances. It is a challenging task to control such a system for getting the desired system output under excessive disturbances and nonlinearities. This led to the intense research in the advancement of robust control methods. Numerous robust control methods are available in the literature[1, 2]. Among these, sliding mode control (SMC) is one of the effectual method used for robust control of the nonlinear system[3−5]. SMC has several important characteristics such as insensitivity to matched uncertainties, simple design and order reduction[6]. SMC uses a discontinuous control input to make the system trajectory to attain and stay on a specific manifold namely, the sliding manifold[7, 8]. SMC consists of two phases, reaching phase and sliding phase. The system state trajectory moves towards the sliding manifold in the reaching phase, whereas it moves along the sliding manifold in the sliding phase[9−13]. In sliding phase, the system performance is completely determined by the sliding manifold design which is insensitive to matched uncertainties and sensitive to unmatched uncertainties. Whereas, in reaching phase, the system is sensitive to disturbances and uncertainties, i.e., robustness cannot be assured in the entire response of the system[14].

The high-frequency switching in SMC makes the system trajectories oscillate quickly about the sliding manifold. This results in chattering. Therefore, the performance deteriorates and causes instability. Moreover, in the conventional SMC design, sliding manifold is chosen in such a way that it has the relative degree of one with respect to the control input, i.e., control input appears in the time derivative of the sliding manifold[5−18]. Preserving the core assets of the conventional SMC, a methodology named higher order SMC (HOSMC) has been used in order to eliminate chattering and restriction on relative degree[19−22]. The HOSMC is the generalization of the conventional SMC in which the control input acts on the higher time derivatives of the sliding manifold[23−25]. The HOSMC is effective in extending the ethical assets of conventional SMC to systems with higher relative degree. It also provides asymptotic convergence of the sliding manifold s and its $(r-1)$-th time derivatives to zero. The asymptotic convergence of the sliding manifold and its time derivatives make the analysis of the overall system difficult. So, the finite time convergence of SMC with any order single input single output (SISO) systems are explained theoretically in [26]. A finite time convergent HOSMC controllers are built based on the homogeneity approach in [23]. The r-th order SMC entails only the information of relative degree r of the system[21, 23]. The discontinuous control developed as a function of sliding manifold s and its consecutive derivatives $\dot{s}, \ddot{s}, \cdots, s^{r-1}$ results in transient chattering. In order to evade this, a quasi-continuous r-th order SMC developed as function of $s, \dot{s}, \ddot{s}, \cdots, s^{r-1}$ is continuous except at the manifold $s = \dot{s} = \ddot{s} = \cdots = s^{r-1} = 0$ of r-th order SMC[27]. If suitably designed, second-order SMC (SOSMC)[28, 29] and HOSMC will provide smooth control with less chattering, better performance and convergence accuracy for a nonlinear system with relative degree higher than one. If the relative degree of a system with respect to the input is one, then Ackerman and Utkin′s formula are used to solve the problem[30]. If relative degree equal to the dimension of the plant and the system is in canonical form, then the

Research Article
Manuscript received December 2, 2016; accepted January 6, 2017; published online June 6, 2017
Recommended by Associate Editor Yuan-Qing Xia

state with the highest relative degree is selected as the sliding variable. However, there is no systematic method for structuring sliding variable in-between the relative degrees as in [30]. The necessary conditions for the existence of sliding manifold is explained in [31]. The design of sliding manifold of any order for a single-input nonlinear system is also described in [31]. At present, there is no general design method for selecting a sliding manifold for a SISO nonlinear systems with specified relative degree and specified sliding-mode dynamics. Also, the control parameters of the SMC have significant impact on control inputs and output regulation performance. Methods like Ziegler-Nichols can be utilized to fine tune the parameters of SMC controller, but they frequently need manual tuning. In order to avoid this manual tuning, various classical optimization methods are available[32−34]. Among these, particle swarm optimization (PSO)[35, 36] is one of the powerful optimization methods that can be easily implemented due to its computational simplicity. The PSO algorithm begins with randomly generating an initial population, which is composed of a number of candidate solutions called particles. In the PSO algorithm, the velocity of a particle is updated based on its own experience and the other particle′s experience[37]. A modified particle swarm optimization (MPSO) based conventional sliding mode control is described in [38]. In [39], a probabilistic PSO (PPSO) is explained. In this paper, a probabilistic particle swarm optimized sliding mode control for output regulation of a SISO nonlinear system with arbitrary relative degree using different sliding manifolds is designed. Also the variation of relative degree with system order and control methodologies for choosing different sliding manifolds are described. The organization of the paper is as follows. Section 2 states the output regulation problem of a SISO nonlinear system. Then, PPSO optimized sliding mode control is explained in Section 3. The controller designs for a nonlinear system with different sliding surfaces using SMC/HOSMC technique are explained with simulation in Section 4. Finally, in Section 5 elaborates the result and analysis, followed by conclusions in Section 6.

2 Problem statement

Consider a SISO nonlinear system:

$$\begin{aligned} \dot{x} &= f(x) + g(x)u \\ y &= h(x) \end{aligned} \tag{1}$$

where $x \in \mathbf{R}^n$ is the state vector which is assumed to be measurable, $u \in \mathbf{R}$ is the control vector and $y \in \mathbf{R}$ is the output vector. $f(x)$, $g(x)$ and $h(x)$ are the smooth vector functions. The objective of the control system is to design a SMC that solves the output regulation problem. The idea behind SMC is to select a sliding manifold s, as a function of the tracking error e such that the trajectory can reach the manifold and stay on it. The tracking error $e \in \mathbf{R}$ is given by

$$e = y - y_d \tag{2}$$

where e is the difference between actual output y and desired values of output y_d. Once the sliding manifold has been defined, then the control law is designed in such a way that it drives the output to the desired value and satisfy (3):

$$s\dot{s} \leq 0. \tag{3}$$

The aim of the SMC is to guarantee that the output always follows the desired trajectory, i.e., error e and its derivative $\dot{e}$ must be zero. sliding surface plays an essential role in describing the dynamics of the system.

2.1 Proportional sliding surface

To fulfil the control objective, the sliding surface is selected in such a way that as surface s goes to zero, the error e also goes to zero. Let the sliding manifold s be

$$s = k_p(y - y_d) \tag{4}$$

where $k_p > 0$ is the proportional gain constant and y_d is the desired output,which is taken as a constant value. Keeping the system states on sliding manifold $s \in \mathbf{R}$ will effect the error e to come close to zero. Therefore, $s = 0$ is a stable sliding manifold, i.e., $e \to 0$ as $t \to \infty$. The derivative of the sliding manifold (4) along the state trajectories of system (1) gives

$$\dot{s} = k_p \frac{\partial h}{\partial x} \left(f(x) + g(x)u \right) = k_p(L_f h(x) + L_g h(x)u) \tag{5}$$

where

$$L_f h(x) = \frac{\partial h}{\partial x} f(x), \; L_g h(x) = \frac{\partial h}{\partial x} g(x)$$

$L_f h(x)$ denotes the Lie derivative of $h(x)$ along a vector field f and $L_g h(x)$ is the Lie derivative of $h(x)$ along a vector field g. According to the sliding mode reaching control law:

$$\dot{s} = -k\text{sgn}(s) \tag{6}$$

where $k > 0$. Combining (5) and (6), the control input u is given as

$$u = \left(k_p L_g h(x) \right)^{-1} \left(-k\text{sgn}(s) - k_p L_f h(x) \right). \tag{7}$$

The control input u appears in the time derivative of s only if $k_p L_g h(x)$ is nonsingular, i.e., the relative degree of the system is one. If system (1) is of relative degree one, then the control input (7) acts on the time derivative of the surface (4) to retain the state trajectories in the sliding surface $s = 0$. The stability of system (1) is analysed by Lyapunov function (8) and its derivative is represented in (9):

$$V = \frac{1}{2}s^2 \tag{8}$$

$$\dot{V} = s\dot{s}. \tag{9}$$

Substituting (7) into (5) yields

$$\dot{V} = -\eta|s| \tag{10}$$

where $\eta = k > 0$ satisfies the inequality condition $s\dot{s} \leq 0$. Then, the system is stable and SMC convergence is assured. Substituting (7) in (1), the system dynamics on the sliding manifold $s = 0$ is given by

$$\dot{x} = f(x) + g(x) \left(k_p L_g h(x) \right)^{-1} (-k\text{sgn}(s) - k_p L_f h(x)). \tag{11}$$

The constraint $s(x) = 0$ decides the system performance on the sliding manifold. Therefore, the movement on the sliding manifold is controlled by the reduced order dynamics $n - 1$.

If $k_p L_g h(x)$ is singular, i.e., the system is of relative degree $r > 1$, then the control input u does not act on the time derivative of s. Hence, the conventional SMC is unable to solve the output regulation problem. Therefore, second order SMC (SOSMC) method is used.

2.1.1 Second order SMC

The SOSMC should satisfy the following condition:

$$s = \dot{s} = 0. \tag{12}$$

If system (1) is of relative degree two, then the control input u steers sliding manifold s and its derivative $\dot{s}$ to zero in finite time and control input u is performing discontinuously on the derivative of $\dot{s}$. The differentiation of $\dot{s}$ with respect to time along the trajectory of system (1) gives

$$\ddot{s} = \frac{\mathrm{d}}{\mathrm{d}t} \left(k_p L_f h(x) + k_p L_g h(x) u \right) = k_p L_f^2 h(x) + k_p L_g L_f h(x) u. \tag{13}$$

The sliding function s and $\dot{s}$ can be made zero in finite time using[31] quasi-continuous control law

$$\ddot{s} = -k \frac{\dot{s} + p|s|^{\frac{1}{2}} \text{sgn}(s)}{|\dot{s}| + p|s|^{\frac{1}{2}}} \tag{14}$$

where $k > 0$ and $p = 1$, which is continuous everywhere except the origin. It becomes zero on the parabola $\dot{s} + |s|^{\frac{1}{2}} \text{sgn}(s)$, for an acceptable value of k. The control input u is obtained by combining (13) and (14) as

$$u = \left(k_p L_g L_f h(x) \right)^{-1} \left(u_s - k_p L_f^2 h(x) \right) \tag{15}$$

where

$$u_s = -k \frac{\dot{s} + |s|^{\frac{1}{2}} \text{sgn}(s)}{|\dot{s}| + |s|^{\frac{1}{2}}}. \tag{16}$$

The control input u acts on the time derivative of $\dot{s}$ only if $L_g L_f h(x)$ is nonsingular, i.e., if the system is of relative degree two, then the output regulation problem for the system is solved by using sliding surface (4).

Substituting (15) in (1), the system dynamics on the sliding manifold $s = 0$ is given by

$$\dot{x} = f(x) + g(x) \left(k_p L_g L_f h(x) \right)^{-1} (u_s - k_p L_f^2 h(x)). \tag{17}$$

The constraints $s(x) = 0, \dot{s}(x) = 0$ decide the system performance on the sliding surface. As a result, sliding manifold motion is controlled by the reduced order dynamics $n - 2$.

If $k_p L_g L_f h(x)$ is singular, i.e., the system is of relative degree $r > 2$, then the control input u does not act on the time derivative of $\dot{s}$. Thus, SOSMC is incapable of solving the output regulation problem of system (1) with relative degree $r > 2$. Hence, HOSMC method is used.

2.1.2 Higher order SMC

HOSMC is the generalisation of conventional SMC. The conditions in HOSMC can be defined as the intersection of the surfaces

$$s = \dot{s} = \ddot{s} = \cdots = s^{r-1} = 0 \tag{18}$$

where r is the order of SMC.

$$\frac{\partial s^r}{\partial u} \neq 0 \tag{19}$$

and

$$K_M \geq \frac{\partial s^r}{\partial u} \geq K_m \geq 0, C \geq |s^r|_{u=0}| \tag{20}$$

where K_M, K_m and $C > 0$. This condition (20) is satisfied at least locally[31]. The goal of the HOSMC design is to obtain the control law so that the system trajectory attains the intersection of manifold (18) in finite time. If system (1) is of relative degree r, then control input u drives s and its $(r-1)$-th time derivatives to zero in finite time. It is performing discontinuously on the r-th time derivative of s. The r-th time derivative of s is given as

$$s^r = k_p L_f^r h(x) + k_p L_g L_f^{r-1} h(x) u. \tag{21}$$

The sliding function s, $\dot{s}$, $\cdots$, s^{r-1} can be made zero in finite time using[31] quasi-continuous control law:

$$s^r = -k \phi_{r-1,r} \left(s, \dot{s}, \ddot{s}, \cdots, s^{r-1} \right) \tag{22}$$

where

$$\phi_{i,r} = \frac{\theta_{i,r}}{N_{i,r}} \tag{23}$$

$$\theta_{i,r} = s^i + p_i N_{(i-1),r}^{\frac{(r-i)}{(r-i+1)}} \tag{24}$$

$$N_{i,r} = |s^i| + p_i N_{(i-1),r}^{\frac{(r-i)}{(r-i+1)}} \tag{25}$$

$$N_{0,r} = |s|, \ \theta_{0,r} = s, \ \phi_{0,r} = \text{sgn}(s). \tag{26}$$

Combining (21) and (22), the control input u is given by

$$u = \left(k_p L_g L_f^{r-1} h(x) \right)^{-1} \left(u_{s1} - k_p L_f^r h(x) \right) \tag{27}$$

where

$$u_{s1} = -k \phi_{r-1,r} \left(s, \dot{s}, \ddot{s}, \cdots, s^{r-1} \right). \tag{28}$$

The control input u appears on s^r only if $k_p L_g L_f^{r-1} h(x)$ is nonsingular, i.e., the system is of relative degree r. Then, output regulation problem for system (1) with relative degree r is solved using r-th order SMC by choosing the surface (4).

The system dynamics on the manifold $s = 0$ is obtained by substituting (27) in (1).

$$\dot{x} = f(x) + g(x) \left(k_p L_g L_f^{r-1} h(x) \right)^{-1} (u_{s1} - k_p L_f^r h(x)). \tag{29}$$

The constraint $s(x), \dot{s}(x), \cdots, s^{r-1} = 0$ decides the system performance on the sliding surface. As a result, the sliding manifold motion is controlled by the reduced order dynamics $n - r$.

Remark 1. If the system is of relative degree r, then the order of the system is reduced to $n - r$ by choosing the sliding manifold (4).

2.2 Proportional integral sliding surface

For improving the robustness of the system, an integral term is included in the sliding manifold (4) resulting in a proportional integral (PI) sliding surface as

$$s = k_p(y - y_d) + k_i \int y - y_d \mathrm{d}t. \tag{30}$$

The differentiation of the sliding manifold (30) along the state trajectories of system (1) gives

$$\begin{aligned}\dot{s} =& \frac{\partial h}{\partial x}\left(k_p(f(x) + g(x)u) \right) + k_i y = \\ & k_p L_f h(x) + k_p L_g h(x)u + k_i h(x).\end{aligned} \tag{31}$$

Combining (31) and (6), the control input u is given by

$$\begin{aligned}u = & \left(k_p L_g h(x) \right)^{-1} (-k\mathrm{sgn}(s) - k_p L_f h(x) - \\ & k_i h(x)).\end{aligned} \tag{32}$$

The control input u acts on the time derivative of s only if $k_p L_g h(x)$ is nonsingular, i.e., system (1) is of relative degree one. Then, the control input (32) drives the system response to the desired value. Therefore, the output regulation problem is solved by choosing the sliding manifold (30).

Substituting (32) in (1), the system dynamics on the sliding manifold $s = 0$ is given as

$$\begin{aligned}\dot{x} =& f(x) + g(x)\left(k_p L_g h(x) \right)^{-1} \\ & (-k\mathrm{sgn}(s) - k_p L_f h(x) - k_i h(x)).\end{aligned} \tag{33}$$

The constraint $s(x) = 0$ decides the system performance on the sliding manifold. Therefore, the movement on the sliding manifold is controlled by the same order dynamics n. Thus, the order of the system remains unchanged in PI based SMC.

If $k_p L_g h(x)$ is singular i.e., the system is of relative degree $r > 1$, then the control input u does not act on the time derivative of s. Hence, conventional SMC is unable to solve the output regulation problem of system (1) with relative degree $r > 1$ using the surface (30). Therefore, SOSMC method is used.

2.2.1 Second order SMC

If system (1) is of relative degree two, then SOSMC is used for solving the output tracking problem. In SOSMC, the control input u drives sliding surface s and its derivative $\dot{s}$ to zero in finite time. It is acting discontinuously on the derivative of $\dot{s}$. The differentiation of $\dot{s}$ with respect to time along the trajectory of system (1) yields

$$\begin{aligned}\ddot{s} =& \frac{\mathrm{d}}{\mathrm{d}t}\left(k_p L_f h(x) + k_p L_g h(x)u + k_i h(x) \right) = \\ & k_p L_f^2 h(x) + k_p L_g L_f h(x)u + k_i L_f h(x) + \\ & k_i L_g h(x)u\end{aligned} \tag{34}$$

where

$$\begin{aligned}L_f^2 h(x) &= L_f L_f h(x) = \frac{\partial (L_f h)}{\partial x} f(x) \\ L_g L_f h(x) &= \frac{\partial (L_f h)}{\partial x} g(x).\end{aligned} \tag{35}$$

Combining (34) and (16), the control input u is obtained as

$$\begin{aligned}u = & \left(k_p L_g L_f h(x) \right)^{-1} (u_s - k_p L_f^2 h(x) - \\ & k_i L_f h(x)).\end{aligned} \tag{36}$$

The control input u acts on the time derivative of $\dot{s}$ only if $k_p L_g L_f h(x)$ is nonsingular and $k_i L_g h(x)$ is singular, i.e., if system (1) is of relative degree two, then SOSMC is used for the output regulation problem of system (1) choosing the surface (30).

Substituting (36) in (1), the system dynamics on the sliding manifold $s = 0$ is given as

$$\begin{aligned}\dot{x} =& f(x) + g(x)\left(k_p L_g L_f h(x) \right)^{-1} \\ & (u_s - k_p L_f^2 h(x) - k_i L_f h(x)).\end{aligned} \tag{37}$$

The constraint $s(x) = 0, \dot{s}(x) = 0$ decides the system performance on the sliding manifold. Therefore, the movement on the sliding manifold is controlled by the reduced order dynamics $n - 1$. If $k_p L_g L_f h(x)$ is singular, i.e., the system is of relative degree $r > 2$, then control input u does not act on the time derivative of $\dot{s}$. Hence, SOSMC is unsuitable for solving the output regulation problem of the system with relative degree $r > 2$. Therefore, HOSMC method is used.

2.2.2 Higher order SMC

If system (1) is of relative degree r, then the r-th time derivative of sliding surface s is

$$s^r = k_p L_f^r h(x) + k_p L_g L_f^{r-1} h(x)u + k_i L_f^{r-1} h(x). \tag{38}$$

The control input u drives sliding manifold s and its $(r-1)$-th time derivative to zero in finite time by acting discontinuously on the r-th time derivative of sliding manifold s. Combining (38) and (28), the control input u is given as

$$\begin{aligned}u = & \left(k_p L_g L_f^{r-1} h(x) \right)^{-1} (u_{s1} - k_p L_f^r h(x) - \\ & k_i L_f^{r-1} h(x)).\end{aligned} \tag{39}$$

The control input u appears in the *r-th* time derivative of sliding surface (s^r) only if $k_p L_g L_f^{r-1} h(x)$ is nonsingular, i.e., system (1) is of relative degree r. Then, the r-th order SMC is used for solving the output regulation problem of system (1) with relative degree r by choosing the surface (30). The system dynamics on the sliding manifold $s = 0$ is obtained by substituting (39) in (1), i.e.,

$$\begin{aligned}\dot{x} =& f(x) + g(x)\left(k_p L_g L_f h(x) \right)^{-1} \\ & (u_s - k_p L_f^2 h(x) - k_i L_f h(x)).\end{aligned} \tag{40}$$

The constraint $s(x), \dot{s}(x), \cdots, s^{r-1} = 0$ decides the system performance on the sliding manifold. As a result, the motion on the sliding manifold is controlled by the reduced order dynamics $n-(r-1)$.

Remark 2. If system (1) is of relative degree r, then the order of the system is reduced to $n-(r-1)$ by choosing the sliding manifold (30).

2.3 Proportional integral derivative surface

For improving the steady state error, a derivative term is included in the PI based sliding manifold, resulting in a proportional integral derivative (PID) based sliding manifold given by

$$s = k_p(y-y_d) + k_i \int (y-y_d)\mathrm{d}t + k_d \frac{\mathrm{d}}{\mathrm{d}t}(y-y_d). \quad (41)$$

The differentiation of the manifold (41) along the state trajectories of system (1) gives

$$\begin{aligned}\dot{s} = \; & k_p L_f h(x) + k_p L_g h(x) u + k_i h(x) + k_d L_f^2 h(x) + \\ & k_d L_g L_f h(x) u \end{aligned} \quad (42)$$

where $k_p > 0$, $k_i > 0$ and $k_d > 0$.

The control u and its derivative $\dot{u}$ appear in the time derivative of s if $k_p L_g h(x)$ and $k_d L_g L_f h(x)$ are nonsingular, i.e., the system is of relative degree one. Then, the output regulation problem is not solved by using the surface (41).

The control input u acts on the time derivative of s if and only if $L_g L_f h(x)$ is nonsingular and $L_g h(x)$ is singular, i.e., the system is of relative degree two. Then, the control input u drives the system response to the desired value, i.e., output regulation problem is solved by choosing the sliding manifold (41). Combining (42) and (6), the control input is given by

$$\begin{aligned} u = \; & (k_d L_g L_f h(x))^{-1} (-k\mathrm{sgn}(s) - k_p L_f h(x) - \\ & k_i h(x) - k_d L_f^2 h(x)). \end{aligned} \quad (43)$$

The dynamics of the system on the sliding manifold $s = 0$ is obtained by substituting (43) in (1), i.e.,

$$\begin{aligned} \dot{x} = & f(x) + g(x)(k_d L_g L_f h(x))^{-1}(-k\mathrm{sgn}(s) - \\ & k_p L_f h(x) - k_i h(x) - k_d L_f^2 h(x)). \end{aligned} \quad (44)$$

The constraint $s(x) = 0$ decides the system performance on the sliding manifold. Therefore, the movement on the sliding manifold is controlled by the same order dynamics n. Hence, the order of the system remains unchanged for the system with relative degree two. If $k_d L_g L_f h(x)$ and $k_p L_g h(x)$ are singular, i.e., the system is of relative degree $r > 2$, then the control input u does not appear in the time derivative of s. Thus, the output regulation problem cannot be solved using conventional SMC. Hence, SOSMC method is used.

2.3.1 Second order SMC

If the system is of relative degree three, second order SMC scheme is used for solving the output tracking problem, then control input u drives sliding manifold s and its time derivative to zero in finite time.

The time derivative of $\dot{s}$ along the trajectory of system (1) yields

$$\begin{aligned} \ddot{s} = \; & k_p L_f^2 h(x) + k_p L_g L_f h(x) u + k_i (L_f h(x) + \\ & L_g h(x) u) + k_d (L_f^3 h(x) + L_g L_f^2 h(x) u). \end{aligned} \quad (45)$$

Control input u appears discontinuously in the time derivative of $\dot{s}$. By combining (45) and (16), the control input u is given by

$$\begin{aligned} u = \; & \left(k_d L_g L_f^2 h(x) \right)^{-1} (u_s - k_p L_f^2 h(x) - \\ & k_i L_f h(x) - k_d L_f^3 h(x)). \end{aligned} \quad (46)$$

The control input u acts on the time derivative of $\dot{s}$ only if $k_d L_g L_f^2 h(x)$ is nonsingular, $k_p L_g L_f h(x)$ and $k_i L_g h(x)$ are singular, i.e., the system is of relative degree three. Then, SOSMC method is used for solving the output regulation problem of the system with relative degree three by choosing the surface (41).

The system dynamics on the sliding manifold $s = 0$ is obtained by substituting (46) in (1), i.e.,

$$\begin{aligned} \dot{x} = & f(x) + g(x) \left(k_d L_g L_f^2 h(x) \right)^{-1} (u_s - \\ & k_p L_f^2 h(x) - k_i L_f h(x) - k_d L_f^3 h(x)). \end{aligned} \quad (47)$$

The constraints $s(x) = 0$, $\dot{s}(x) = 0$ decide the system performance on the sliding manifold, therefore the movement on the sliding manifold is controlled by the reduced order dynamics $n-1$.

If $k_d L_g L_f^2 h(x)$ is singular, i.e., the relative degree of the system $r > 3$, then control input u is not acting on the time derivatives of $\dot{s}$. Thus, SOSMC method is incapable of solving the output regulation problem of the system with relative degree $r > 3$. Hence, HOSMC method is used.

2.3.2 Higher order SMC

The intention of the HOSMC method is to obtain the control input so that the system trajectory attains the intersection of surface (18) in finite time. If the system is of relative degree r, then the control input u drives sliding surface s and its $(r-2)$-th time derivatives to zero in finite time and it is acting discontinuously on the $(r-1)$-th time derivative of sliding surface. The $(r-1)$-th time derivative of sliding manifold s is given as

$$\begin{aligned} s^{r-1} = \; & k_p L_f^{r-1} h(x) + k_p L_g L_f^{r-2} h(x) u + \\ & k_i L_f^{r-2} h(x) + k_i L_g L_f^{r-3} h(x) u + \\ & k_d L_f^r h(x) + k_d L_g L_f^{r-1} h(x) u. \end{aligned} \quad (48)$$

The control input u is obtained by combining (48) and (28), i.e.,

$$\begin{aligned} u = \; & \left(k_d L_g L_f^{r-1} h(x) \right)^{-1} (u_{s1} - k_p L_f^{r-1} h(x) - \\ & k_i L_f^{r-2} h(x) - k_d L_f^r h(x)). \end{aligned} \quad (49)$$

The control input u appears in $(r-1)$-th time derivative of sliding surface (s^{r-1}) only if $k_d L_g L_f^{r-1} h(x)$ is nonsingular and $k_p L_g L_f^{r-2} h(x)$, $k_i L_g L_f^{r-3} h(x)$ are singular, i.e., the system is of relative degree r. Then, output regulation

problem for a system with relative degree r is solved using $(r-1)$-th order SMC by choosing the surface (41).

The dynamics of the system on the sliding manifold $s=0$ is obtained by substituting (49) in (1).

$$\dot{x} = f(x) + g(x)\left(k_d L_g L_f^{r-1} h(x)\right)^{-1}(u_{s1} - k_p L_f^{r-1} h(x) - k_i L_f^{r-2} h(x) - k_d L_f^r h(x)). \quad (50)$$

The constraint $s(x), \dot{s}(x), \cdots, s^{r-2} = 0$ decides the system performance on the sliding manifold. Therefore, the movement on the sliding manifold is controlled by the reduced order dynamics $n-(r-2)$.

Remark 3. If the system is of relative degree r, then the order of the system is reduced to $n-(r-2)$ by choosing the sliding surface (41).

3 PPSO optimized sliding mode control

Optimization of control parameters is always considered as a challenge. In order to obtain a stable and efficient control system, these parameters are very crucial. Majority of the control parameters are adjusted by conventional methods, which are difficult and time consuming. This paper introduces a novel method which employs swarm intelligence for optimizing the control parameters of SMC. Particle swarm optimization (PSO) was originally proposed by Kennedy and Eberhart[35] in 1995 influenced by the social behavior of birds or fish flocking. The probable solution in a PSO algorithm acts as a particle and the swarm behavior of the natural creatures is simulated to attain the optimum solution. The migrations of the particles in the search space are guided by its initial position and velocity vectors. The velocity vectors are responsible for directing the trajectory of the particle and the positions of these particles are modified based on this velocity. The fitness value of each particle is evaluated by its fitness function. Based on the fitness value, the velocity and position of each particle are updated. Individual particles are attracted towards their previous best position and the swarm′s best position in the search space, leads them towards the optimal position[36]. The fitness function used in this work is the integral square error (ISE)$=\int e^2 \mathrm{d}t$. This is reflected by the system time constant, which decides the performance of any nonlinear system.

In PSO, the introduction of a random function will lead to limited probabilistic displacement since the velocity of each particle is the resultant of P_{best} and g_{best}. So, the traditional PSO is sometimes incapable of searching a solution space effectively and expeditiously. This leads to a decrease in convergence rates and precision of PSO. To overcome this, probabilistic particle swarm optimization (PPSO) method[39] is proposed in which the velocity of each particle is updated with respect to a probability either towards particle best (P_{best}) or global best (g_{best}). In the PPSO approach, the particle direction of movement is towards P_{best} or g_{best} depending on the movement probability, which assists the particle to attain global or local optima efficiently leading to a large branch out of solution. In PPSO, the movements of P_{best} and g_{best} are given in (51) and (52) subjected to the constraints (53) and (54). P_{best} movement

$$\begin{aligned} v_i^{k+1} &= w v_i^k + c_1 rand(x_{Pbest} - x_i^k) \\ x_i^{k+1} &= x_i^k + v_i^{k+1} \end{aligned} \quad (51)$$

g_{best} movement

$$\begin{aligned} v_i^{k+1} &= w v_i^k + c_2 rand(x_{gbest} - x_i^k) \\ x_i^{k+1} &= x_i^k + v_i^{k+1}. \end{aligned} \quad (52)$$

The constraints are

$$\begin{aligned} v_i^{k+1} &= v_{\max}, \quad \text{if} \quad v_i^{k+1} \geq v_{\max} \\ v_i^{k+1} &= v_{\min}, \quad \text{if} \quad v_i^{k+1} \leq v_{\min} \end{aligned} \quad (53)$$

$$\begin{aligned} x_i^{k+1} &= x_{\min}, \quad \text{if} \quad x_i^{k+1} < x_{\min} \\ x_i^{k+1} &= x_{\max}, \quad \text{if} \quad x_i^{k+1} > x_{\max}. \end{aligned} \quad (54)$$

The flowchart of the PPSO based SMC of the nonlinear system is shown in Fig. 1.

In the diagram, P_i is the random number generated between 0 and 1 associated with each particle and this is examined with displacement probability P_{mov}. If $P_{mov} \leq P_i$ then, perform P_{best} movement. Otherwise, perform g_{best} movement. In proportional surface based SMC, the major task is to optimize the parameters k_p in (4) and k in (7) simultaneously by PPSO algorithm. Initially, these parameters are taken as random values, such that $k_p > 0$ and $k > 0$. After "n" number of iterations, optimized parameter value (g_{best} value) for k_p in (4) and k in (7) are obtained from PPSO, when it satisfies the objective function. These optimized parameters values, i.e., k_p and k are given to P based SMC controller.

In proportional integral (PI) surface based SMC, the major task is to optimize the parameters k_p and k_i in (30) and k in (32) simultaneously by PPSO algorithm. Initially, these parameters are taken as random values, such that $k_p > 0$, $k_i > 0$, $k_d > 0$ and $k > 0$. After "n" number of iterations, optimized parameters values (g_{best} value) for k_p and k_i in (30) and k in (32) are obtained from PPSO, when it satisfies the objective function. These optimized parameters values, i.e., k_p, k_i and k are given to PI based SMC controller.

In PID surface based SMC, the major task is to optimize the parameters k_p, k_i, k_d in (41) and k in (43) simultaneously by PPSO algorithm. Initially, these parameters are taken as random values, such that $k_p > 0$, $k_i > 0$, $k_d > 0$ and $k > 0$. After "n" number of iterations, optimized parameters values (g_{best} value) for k_p, k_i and k_d in (41) and k in (43) are obtained from PPSO, when it satisfies the objective function. The block diagram of PPSO optimized SMC of an uncertain nonlinear system using PID surface is shown in Fig. 2.

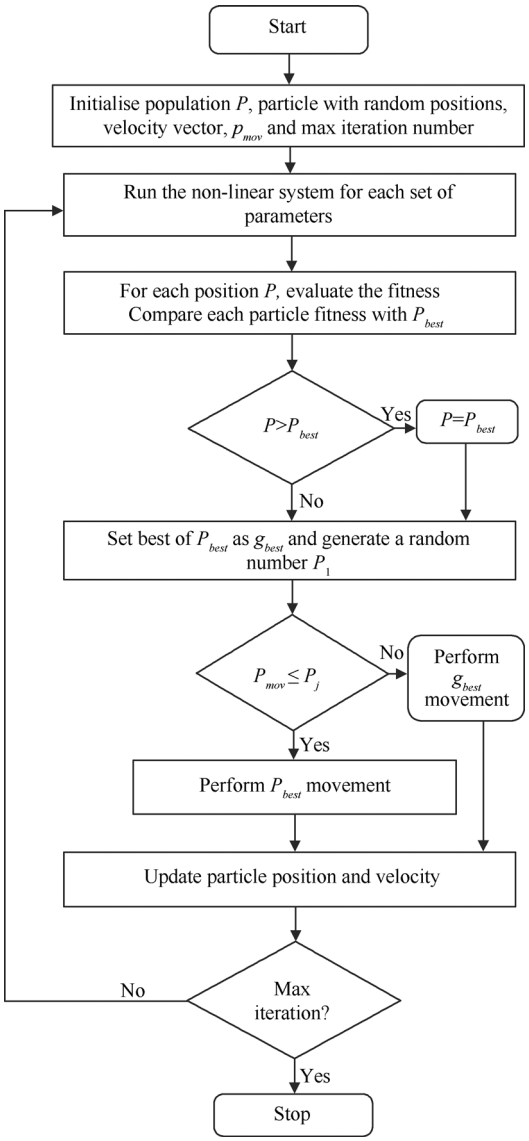

Fig. 1. Flowchart of PPSO optimised SMC of SISO nonlinear system

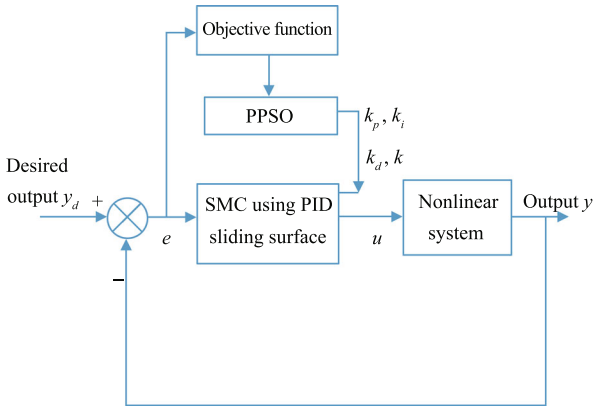

Fig. 2. Block diagram of PPSO optimized SMC of the nonlinear system using PID surface

The objective of PPSO is to minimize the objective function/fitness function as the ISE. So, the error e as in (2) is given to PPSO and SMC algorithm. The PID based SMC controller produces the control signal by using these optimized control parameters k_p, k_i and k_d in (41) and k in (43) and it is given to the nonlinear system to get the desired output.

4 Numerical simulation

The goal is to design a SMC using PID based sliding surface for regulating the output of a nonlinear system with an arbitrary relative degree to the desired value. The desired value is assumed to be zero. The simulation results are compared with output tracking of nonlinear system with arbitrary relative degree using SMC with P and PI based sliding surfaces. Consider a 4th order nonlinear system as

$$\begin{aligned} \dot{x_1} &= x_2 \\ \dot{x_2} &= x_3 \\ \dot{x_3} &= x_4 \\ \dot{x_4} &= x_2^2 + x_1^2 + \sin(x_3) + u. \end{aligned} \tag{55}$$

4.1 Nonlinear system with relative degree one

In the simulation of SMC of nonlinear system (55) with relative degree one, the output y is taken as x_4. The sliding surface (4) and conventional SMC (7) for system (55) is of relative degree one using P based sliding surface and are given by

$$\begin{aligned} s &= k_p x_4 \\ u &= k_p^{-1}\big(- k\mathrm{sgn}(s) - k_p(x_2^2 + x_1^2 + \sin(x_3))\big). \end{aligned} \tag{56}$$

The sliding surface (30) and conventional SMC (36) for system (55) with relative degree one using PI based sliding surface are given as

$$\begin{aligned} s &= k_p x_4 + k_i \int x_4 \\ u &= k_p^{-1}\big(- k\mathrm{sgn}(s) - k_p(x_2^2 + x_1^2 + \sin(x_3)) - k_i x_4\big). \end{aligned} \tag{57}$$

The system output response y, control input u, tracking error e and sliding surface s for system (55) with relative degree one using P and PI based sliding surfaces are shown in Fig. 3.

4.2 Nonlinear system with relative degree two

In the simulation of SMC of nonlinear system (55) with relative degree two, the output y is taken as x_3. The sliding surface (4), its time derivative and SOSMC control (15) for system (55) with relative degree two using P based sliding surface are given as

$$\begin{aligned} s &= k_p x_3, \ \ \dot{s} = k_p x_4 \\ u &= k_p^{-1}\big(u_s - k_p(x_2^2 + x_1^2 + \sin(x_3)\big). \end{aligned} \tag{58}$$

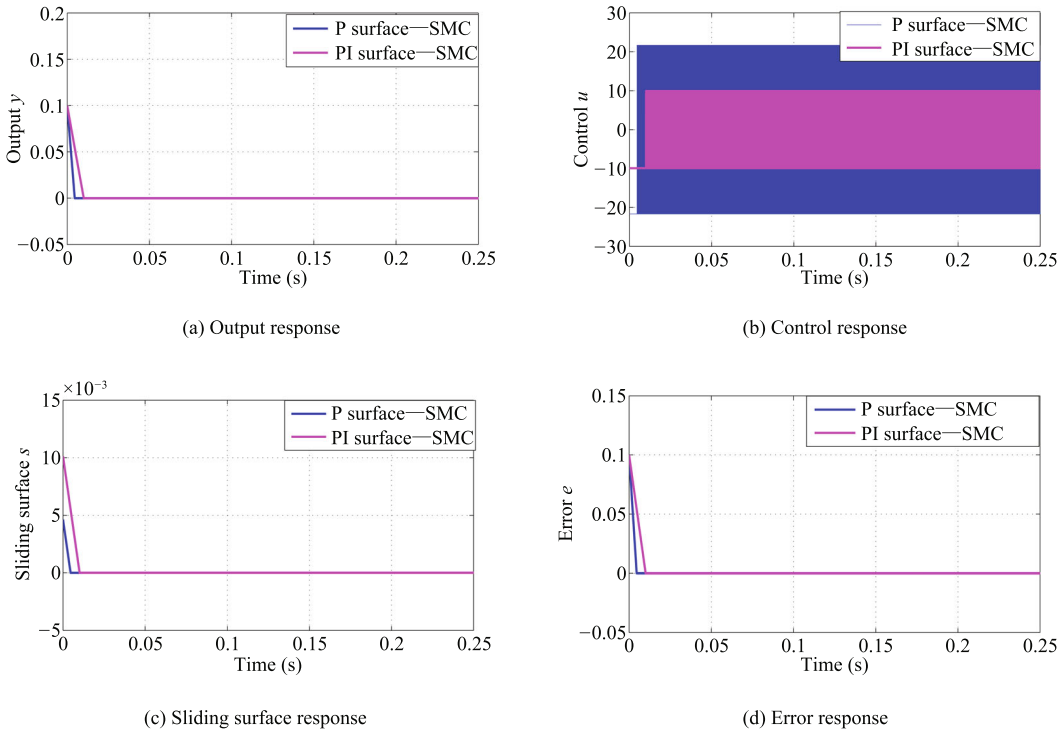

(a) Output response

(b) Control response

(c) Sliding surface response

(d) Error response

Fig. 3 Simulation of SMC of system (55) with relative degree one using P and PI based sliding surfaces(Color versions of figures in this paper are available online.)

The sliding surface (30) and SOSMC control (36) for system (55) with relative degree two using PI based sliding surface are given by

$$s = k_p x_3 + k_i \int x_3,\ \dot{s} = k_p x_4 + k_i x_3$$
$$u = k_p^{-1}\big(u_s - k_p(x_2^2 + x_1^2 + \sin(x_3)) - k_i x_4\big). \tag{59}$$

The sliding surface (41) and conventional SMC control (43) for system (55) with relative degree two using PID based sliding surface are given as

$$s = k_p x_3 + k_i \int x_3 + k_d \dot{x_3}$$
$$u = k_d^{-1}\big(-k\text{sgn}(s) - k_p x_4 - k_i x_3 - k_d(x_2^2 + x_1^2 + \sin(x_3))\big). \tag{60}$$

The system output y, the control input u, tracking error e, sliding surface s, derivative of error $(\dot{e})$ versus error (e) and derivative of surface $(\dot{s})$ versus surface (s) responses for system (55) with relative degree two using P, PI based SOSMC and PID based conventional SMC are shown in Fig. 4.

4.3 Nonlinear system with relative degree three

In the simulation of SMC of system (55) with relative degree three, the output y is taken as x_2. The sliding surface (4) and its derivatives for system (55) with relative degree three using P based sliding surface are given as

$$s = k_p x_2,\ \dot{s} = k_p x_3,\ \ddot{s} = k_p x_4. \tag{61}$$

The HOSMC control (27) for system (55) with relative degree three using P based sliding surface are given by

$$u = k_p^{-1}\big(u_{s1} - k_p(x_2^2 + x_1^2 + \sin(x_3))\big) \tag{62}$$

where u_{s1} for relative degree three is

$$u_{s1} = -k\frac{\big(\ddot{s} + 2\big(|\dot{s}| + |s|^{\frac{2}{3}}\big)^{-\frac{1}{2}}(\dot{s} + |s|^{\frac{2}{3}}\sin(s))\big)}{\big(\ddot{s} + 2(|\dot{s}| + |s|^{\frac{2}{3}})^{\frac{1}{2}}\big)}. \tag{63}$$

The sliding surface (30) and HOSMC control (39) for system (55) with relative degree three using PI based sliding surface are given as

$$s = k_p x_2 + k_i \int x_2,\ \dot{s} = k_p x_3 + k_i x_2$$
$$\ddot{s} = k_p x_4 + k_i x_3 \tag{64}$$

$$u = k_p^{-1}\big(u_{s1} - k_p(x_2^2 + x_1^2 + sin(x_3)) - k_i x_4\big). \tag{65}$$

The sliding surface (41), its time derivative and SOSMC control (46) for system (55) with relative degree three us-

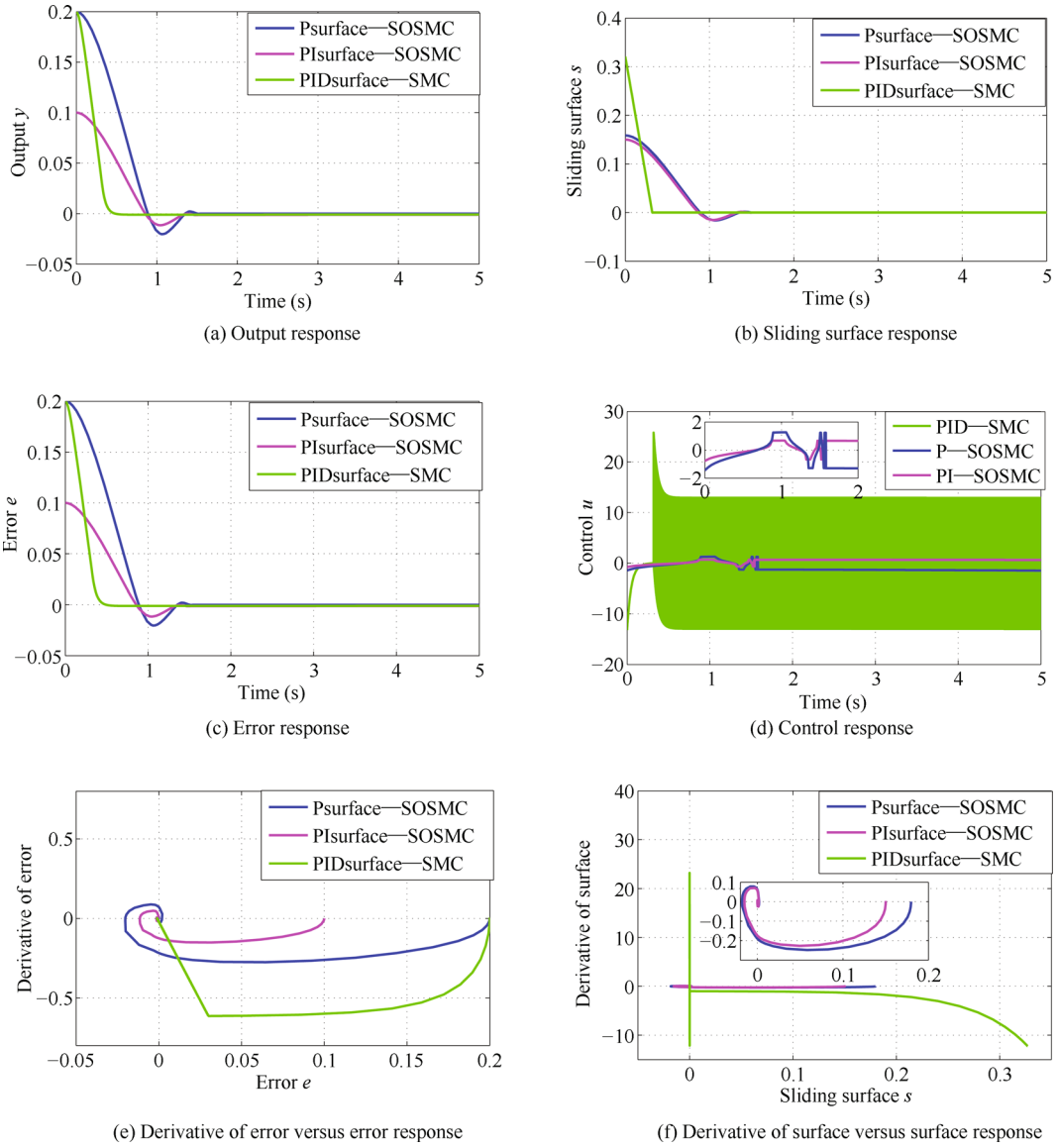

(a) Output response (b) Sliding surface response

(c) Error response (d) Control response

(e) Derivative of error versus error response (f) Derivative of surface versus surface response

Fig. 4 Simulation of P, PI based SOSMC and PID based conventional SMC of system (55) with relative degree two

ing PID based sliding surface are given by

$$s = k_p x_2 + k_i \int x_2 + k_d \dot{x}_2$$

$$\dot{s} = k_p x_3 + k_i x_2 + k_d x_4 \tag{66}$$

$$u = k_d^{-1}(u_s - k_p x_4 - k_i x_3 - k_d(x_2^2 + x_1^2 + \sin(x_3))). \tag{67}$$

The system output y, error e, control input u, sliding surface s, derivative of surface ($\dot{s}$) versus surface (s) and derivative of error ($\dot{e}$) versus error (e) responses for system (55) with relative degree three using P, PI based HOSMC and PID based SOSMC are shown in Fig. 5.

In all the simulations, PPSO method is used for optimizing the control parameters. The parameters used for PPSO techniques in the simulation are listed in Table 1.

Table 1 Parameters used for PPSO techniques in the simulation

Parameters	Relative degree	P surface	PI surface	PID surface
Particle number	1, 2, 3	6	6	6
$w_{\max}$	1, 2, 3	0.9	0.9	0.9
$w_{\min}$	1, 2, 3	0.4	0.4	0.4
$c_{1\,\max}$	1, 2, 3	2	2	2
$c_{1\,\min}$	1, 2, 3	0.1	0.1	0.1
$c_{2\,\max}$	1, 2, 3	2	2	2
$c_{2\,\min}$	1, 2, 3	0.1	0.1	0.1
P_{mov}	1, 2, 3	0.7	0.7	0.7
	1	10	20	–
Iteration number	2	20	20	20
	3	25	25	20

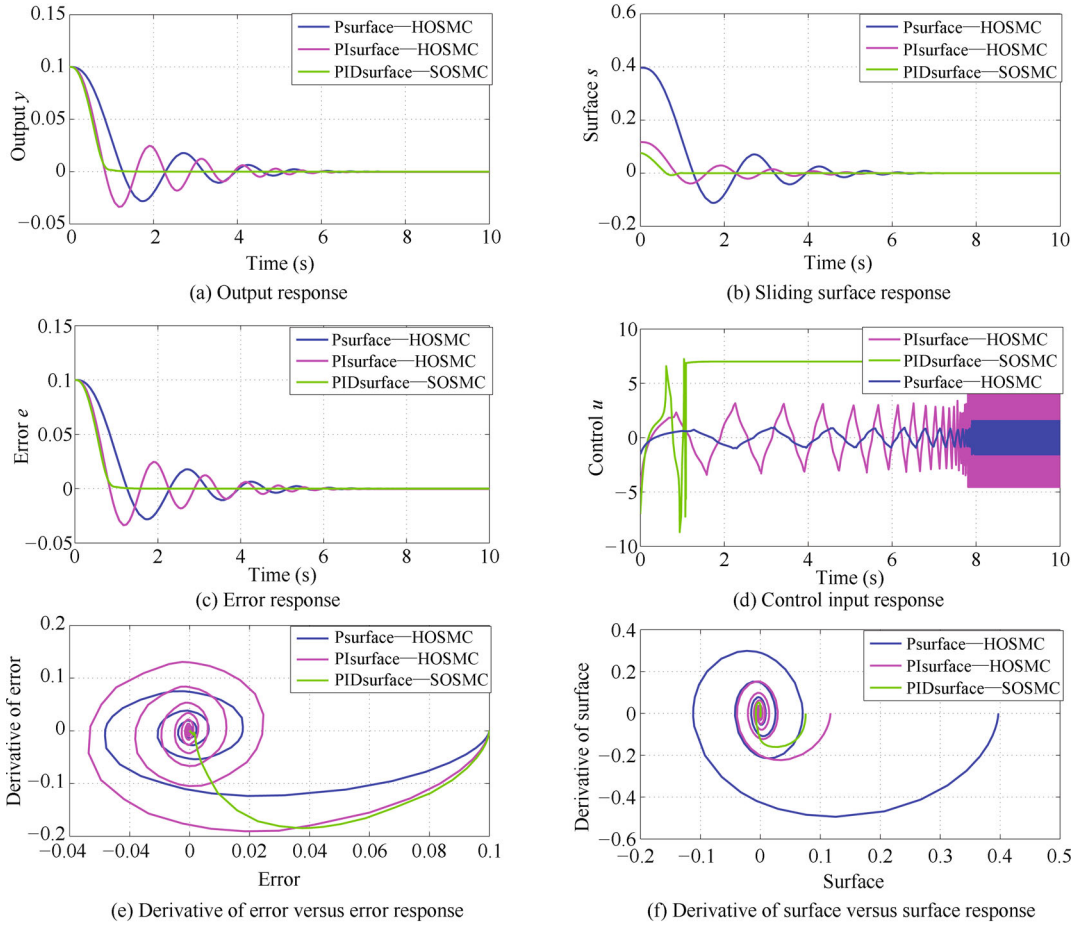

Fig. 5 Simulation of P, PI based HOSMC and PID based SOSMC of system (55) with relative degree three

The SMC control parameters obtained from PPSO techniques for the simulation is given in Table 2.

4.4 System uncertainties and disturbance

By considering system parameter uncertainties and disturbance, system (55) has been modified as

$$\begin{aligned} \dot{x_1} &= 2x_2 \\ \dot{x_2} &= 3x_3 \\ \dot{x_3} &= 4x_4 \\ \dot{x_4} &= x_2^2 + x_1^2 + \sin(x_3) + u + d. \end{aligned} \tag{68}$$

5 Results and discussion

In this work, a comparative analysis of a nonlinear system using different sliding surface is studied. The results of mathematical analysis and simulation for a nonlinear system with different relative degree using different sliding surfaces are explained as follows.

5.1 Mathematical analysis

The mathematical analysis of system (1) for P, PI and PID based sliding surface is shown in Table 3. It is observed that as the relative degree of the system increases from 1 to r for P based sliding surface, the corresponding order of the system changes from $n-1$ to $n-r$. Then, the control method changes from SMC to HOSMC respectively as shown in Table 3.

Table 2 Optimized SMC parameters used for the simulation

Control parameters	Relative degree	P surface	PI surface	PID surface
k	1	1.002 4	1.001 4	–
	2	1.001 7	1.002 9	1.002 9
	3	6.100 0	5.300 0	1.001 6
k_p	1	0.048 5	0.097 0	–
	2	0.859 9	1.499 2	1.614 1
	3	3.947 4	1.165 1	0.752 6
k_i	1	–	0.028 7	–
	2	–	0.042 5	0.041 5
	3	–	$9.545\,7 \times 10^{-4}$	$5.396\,5 \times 10^{-4}$
k_d	2	–	–	0.071 3
	3	–	–	0.135 3

In the case of PI based sliding surface, it is observed that if the relative degree of the system increases from 1 to r,

then the corresponding order of the system is reducing from n to $n-(r-1)$ and the control method changes from SMC to HOSMC respectively as shown in Table 3.

In PID based sliding surface, it is observed that if the relative degree of the system increases from 1 to r, then corresponding order of the system reduces from n to $n-(r-2)$ and the control method changes from SMC to HOSMC respectively as shown in Table 3. It is also observed that the order of the system remains the same for PI based sliding surface with relative degree one and PID based sliding surface with relative degree two.

Table 3 Relative degree, system order and control method for choosing different sliding surfaces

Surface	Relative degree	Control method	System. order
P-surface	1	SMC	$n-1$
	2	SOSMC	$n-2$
	⋮	⋮	⋮
	r	HOSMC	$n-r$
PI-surface	1	SMC	n
	2	SOSMC	$n-1$
	⋮	⋮	⋮
	r	HOSMC	$n-(r-1)$
PID-surface	2	SMC	n
	3	SOSMC	$n-1$
	⋮	⋮	⋮
	r	HOSMC	$n-(r-2)$

5.2 Simulation analysis

If system (55) is of relative degree one, then P and PI based SMC is used for regulating the output of the system as shown in Fig. 3. It is observed from Figs. 3 (a), 3 (c) and 3 (d) that, P based SMC output, surface and error responses converge to zero in 0.005 s whereas, in the case of PI based SMC, they converge to zero in 0.01 s. From Fig. 3 (b), it is observed that control input in P based SMC showed chattering between +20 and −20 while, in PI based SMC, the chattering is between +10 and −10 with reduced control gain k as shown in Table 2. From this analysis, PI based sliding surface design is preferred when the system is of relative degree one, since the control input has less chattering with reduced control gain k. If system (55) is of relative degree two, then P, PI based SOSMC and PID based conventional SMC are used for regulating the output of the system as shown in Fig. 4. It is noticed from Fig. 4 (a) and 4 (c) that P based SOSMC output and error responses converge to zero in 1.4 s with an overshoot of −0.02. In the case of PI based SOSMC, the output and error responses converge to zero in 1.3 s with an overshoot of −0.01, and for PID based SMC, they converge to zero in 0.4 s without any overshoot. PID based SMC surface converges to zero faster than P and PI based SOSMC as given in Fig. 4 (b). It is also noticed from Fig. 4 (d) that PID based SMC control input is chattering between −12 and +12, whereas P and PI based SOSMC produces continuous control input with less chattering. The $\dot{e}$ versus e and $\dot{s}$ versus s responses are shown in Figs. 4 (e) and 4 (f) respectively. It is observed that PI based SOSMC reaching phase is reduced much greater than P based SOSMC and PID based SMC. By considering the simulation results of system (55), it is concluded that PI based sliding surface design is preferred when the relative degree of the system is two, since the control input is continuous with reduced reaching phase. If system (55) is of relative degree three, then P, PI based HOSMC and PID based SOSMC are used for regulating the output of the system as shown in Fig. 5. It is noticed from Figs. 5 (a) and 5 (c) that the output and the error responses of P and PI based HOSMC converge to zero in 6 s and 5.8 s respectively. However, in PID based SOSMC, the output and the error responses converge to zero in 1 s with reduced control parameters (Table 2). It is observed that in PID based SOSMC, sliding surface s and $\dot{s}$ versus s converges faster than P and PI based HOSMC as shown in Figs. 5 (b) and 5 (f). It is also observed from Fig. 5 (d) that PID based SOSMC control input is continuous whereas, P based HOSMC control input is continuous up to 8 s and PI based HOSMC is continuous up to 7.8 s. The $\dot{e}$ versus e and $\dot{s}$ versus s response is shown in Figs. 5 (e) and 5 (f) respectively. It is noticed from Figs. 5 (e) and 5 (f) that in PID based SOSMC, reaching phase is reduced much greater than P and PI based HOSMC. From this analysis, it is concluded that PID based sliding surface design is effective for higher relative degree since the control input is continuous with reduced reaching phase.

From Fig. 6, it is noted that system (68) is robust to parameter uncertainties and disturbance. It also shows the regulation of output with time varying desired output. From Figs. 6 (a) to 6 (d), it is revealed that for the system with relative degree two, PID based sliding surface is more robust to disturbance and uncertainties compared with P and PI surface.

6 Conclusions

This paper explains the design of sliding mode control for SISO system with different sliding surfaces such as P, PI and PID. These sliding surfaces are designed based on the relative degree of the system to be controlled. The controller parameters are tuned based on an optimization technique called probabilistic particle swarm optimization. It is shown that the reduced order dynamics of the system on the sliding manifold is more for PID based sliding surface compared to P and PI. However, the performance of the PID based sliding surface design is better for a system with higher relative degree. A detailed comparison is presented with the help of numerical simulations. Different optimization techniques for various sliding surfaces can be considered as a future work.

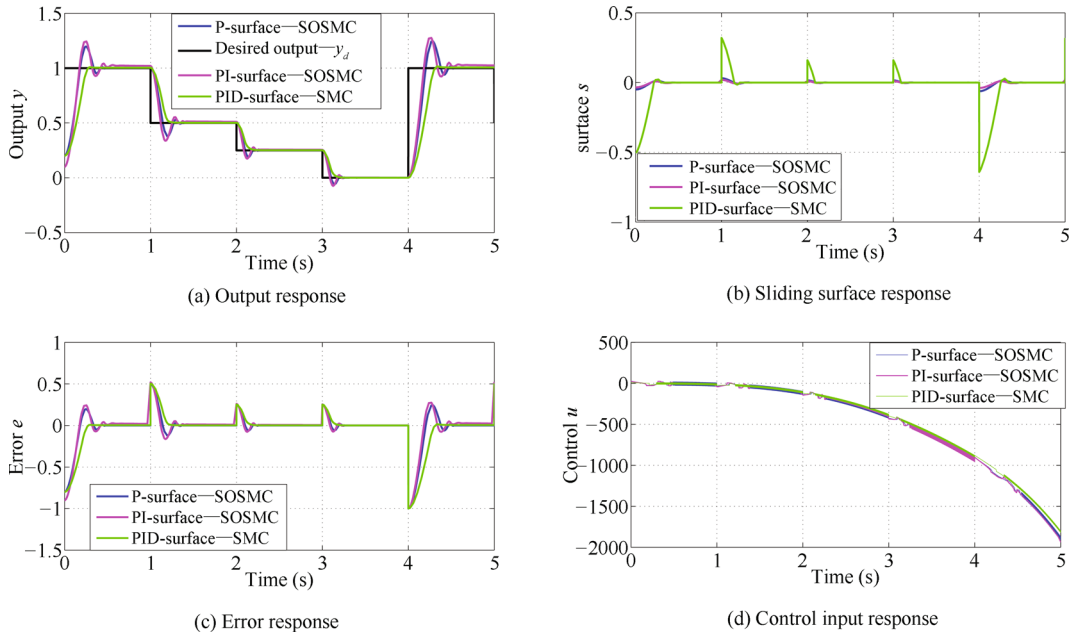

(a) Output response

(b) Sliding surface response

(c) Error response

(d) Control input response

Fig. 6 Simulation of P, PI based SOSMC and PID based conventional SMC of system (68) with relative degree two

References

[1] M. Allouche, M. Chaabane, M. Souissi, D. Mehdi, F. Tadeo. State feedback tracking control for indirect field-oriented induction motor using fuzzy approach. *International Journal of Automation and Computing*, vol. 10, no. 2, pp. 99–110, 2013.

[2] X. C. Shi, T. P. Zhang. Adaptive tracking control of uncertain MIMO nonlinear systems with time-varying delays and unmodeled dynamics. *International Journal of Automation and Computing*, vol. 10, no. 3, pp. 194–201, 2013.

[3] V. I. Utkin. *Sliding Modes in Control and Optimization: Communications and Control Engineering Series*, Berlin, Heidelberg, Germany: Springer, 1992.

[4] C. Edwards, S. Spurgeon. *Sliding Mode Control: Theory and Applications*, Florida, USA: CRC Press, 1998.

[5] F. Li, H. L. Xie. Sliding mode variable structure control for visual servoing system. *International Journal of Automation and Computing*, vol. 7, no. 3, pp. 317–323, 2010.

[6] V. Utkin, J. Guldner, J. X. Shi. *Sliding Mode Control in Electro-Mechanical Systems*, 2nd ed., Florida, USA: CRC Press, vol. 34, 2009.

[7] L. Fridman, A. Levant. High order sliding mode. *Sliding Mode Control in Engineering*, W. Perruquetti, J. P. Barbot, Eds., New York, USA: Marcel Dekker, pp. 53–101, 2002.

[8] S. C. Chung, C. L. Lin. A general class of sliding surface for sliding mode control. *IEEE Transactions on Automatic Control*, vol. 43, no. 1, pp. 115–119, 1998.

[9] A. Levant. Sliding order and sliding accuracy in sliding mode control. *International Journal of Control*, vol. 58, no. 6, pp. 1247–1263, 1993.

[10] B. Bandyopadhyay, A. G. E. Abera, S. Janardhanan, V. Sreeram. Sliding mode control design via reduced order model approach. *International Journal of Automation and Computing*, vol. 4, no. 4, pp. 329–334, 2007.

[11] L. Zouari, H. Abid, M. Abid. Sliding mode and PI controllers for uncertain flexible joint manipulator. *International Journal of Automation and Computing*, vol. 12, no. 2, pp. 117–124, 2015.

[12] W. J. Cao, J. X. Xu. Nonlinear integral-type sliding surface for both matched and unmatched uncertain systems. *IEEE Transactions on Automatic Control*, vol. 49, no. 8, pp. 1355–1360, 2004.

[13] F. Castanos, L. Fridman. Analysis and design of integral sliding manifolds for systems with unmatched perturbations. *IEEE Transactions on Automatic Control*, vol. 51, no. 5, pp. 853–858, 2006.

[14] V. Utkin, J. X. Shi. Integral sliding mode in systems operating under uncertainty conditions. In *Proceedings of the 35th Conference on Decision and Control*, IEEE, Kobe, Japan, vol. 4, pp. 4591–4596, 1996.

[15] H. Sira-Ramirez. A relative degree approach for the control in sliding mode of nonlinear systems of general type. In *Proceeding of the 1st International Workshop on Variable Structure Systems and Their Applications*, pp. 29–51, 1990.

[16] A. Isidori. *Nonlinear Control Systems: An Introduction*. Berlin Heidelberg, Germany: Springer, 2013.

[17] H. Sira-Ramirez. Nonlinear variable structure systems in sliding mode: The general case. *IEEE Transactions on Automatic Control*, vol. 34, no. 11, pp. 1186–1188, 1989.

[18] H. Sira-Ramirez. Sliding regimes in general non-linear systems: A relative degree approach. *International Journal of Control*, vol. 50, no. 4, pp. 1487–1506, 1989.

[19] T. Defoort, A. Floquet, A. Kokosy, W. Perruquetti. A novel higher order sliding mode control scheme. *Systems & Control Letters*, vol. 58, no. 2, pp. 102–108, 2009.

[20] S. Laghrouche, F. Plestan, A. Glumineau. Higher order sliding mode control based on integral sliding mode. *Automatica*, vol. 43, no. 3, pp. 531–537, 2007.

[21] A. Levant. Higher-order sliding modes, differentiation and output-feedback control. *International Journal of Control*, vol. 76, no. 9–10, pp. 924–941, 2003.

[22] F. Dinuzzo, A. Ferrara. Higher order sliding mode controllers with optimal reaching. *IEEE Transactions on Automatic Control*, vol. 54, no. 9, pp. 2126–2136, 2009.

[23] A. Levant. Homogeneity approach to high-order sliding mode design. *Automatica*, vol. 41, no. 5, pp. 823–830, 2005.

[24] R. Ling, M. R. Wu, Y. Dong, Y. Chai. High order sliding-mode control for uncertain nonlinear systems with relative degree three. *Communications in Nonlinear Science and Numerical Simulation*, vol. 17, no. 8, pp. 3406–3416, 2012.

[25] A. Levant, L. Alelishvili. Integral high-order sliding modes. *IEEE Transactions on Automatic Control*, vol. 52, no. 7, pp. 1278–1282, 2007.

[26] A. Levant. Universal single-input-single-output (SISO) sliding-mode controllers with finite-time convergence. *IEEE Transactions on Automatic Control*, vol. 46, no. 9, pp. 1447–1451, 2001.

[27] A. Levant. Quasi-continuous high-order sliding-mode controllers. *IEEE Transactions on Automatic Control*, vol. 50, no. 11, pp. 1812–1816, 2005.

[28] H. Romdhane, K. Dehri, A. S. Nouri. Second order sliding mode control for discrete decouplable multivariable systems via input-output models. *International Journal of Automation and Computing*, vol. 12, no. 6, pp. 630–638, 2015.

[29] S. Mahjoub, F. Mnif, N. Derbel. Second-order sliding mode approaches for the control of a class of underactuated systems. *International Journal of Automation and Computing*, vol. 12, no. 2, pp. 134–141, 2015.

[30] D. Hernández, F. Castaños, L. Fridman. Pole-placement in higher-order sliding-mode control. In *Proceedings of the 19th World Congress International Federation of Automatic Control, Cape Town, South Africa*, pp. 1386–1391, 2014.

[31] V. Muralidharan, A. D. Mahindrakar, V. Sankaranarayanan. A Constructive method for designing higher order sliding surfaces for single-input nonlinear system. *IFAC Proceedings Volumes*, vol. 44, no. 1, pp. 3944–3949, 2011.

[32] Y. J. Liu, Y. Gao, S. C. Tong, Y. M. Li. Fuzzy approximation-based adaptive backstepping optimal control for a class of nonlinear discrete-time systems with dead-zone. *IEEE Transactions on Fuzzy Systems*, vol. 24, no. 1, pp. 16–28, 2016.

[33] Y. Gao, Y. J. Liu. Adaptive fuzzy optimal control using direct heuristic dynamic programming for chaotic discrete-time system. *Journal of Vibration and Control*, vol. 22, no. 2, pp. 595–603, 2014.

[34] Y. J. Liu, L. Tang, S. C. Tong, C. L. P. Chen, D. J. Li. Reinforcement learning design-based adaptive tracking control with less learning parameters for nonlinear discrete-time MIMO systems. *IEEE Transactions on Neural Networks and Learning Systems*, vol. 26, no. 1, pp. 165–176, 2015.

[35] J. Kennedy, R. Eberhart. Particle swarm optimization. *Proceedings of IEEE International Conference on Neural Networks*, IEEE, Perth, Myanmar, vol. 4, pp. 1942–1948, 1995.

[36] M. H. T. Omar, W. M. Ali, M. Z. Mostafa. Auto tuning of PID controller using swarm intelligence. *International Review of Automatic Control*, vol. 4, no. 3, pp. 319–327, 2011.

[37] Z. L. Gaing. A particle swarm optimization approach for optimum design of PID controller in AVR system. *IEEE Transactions on Energy Conversion*, vol. 19, no. 2, pp. 384–391, 2004.

[38] Z. M. Chen, W. J. Meng, J. G. Zhang, J. C. Zeng. Scheme of sliding mode control based on modified particle swarm optimization. *Systems Engineering-Theory & Practice*, vol. 29, no. 5, pp. 137–141, 2009.

[39] K. Sundereswaran, V. Devi. Application of a modified particle swarm optimization technique for output voltage regulation of boost converter. *Electric Power Components and Systems*, vol. 39, no. 3, pp. 288–300, 2011.

M. S. Sunila received the B. Tech. degree in electrical and electronics engineering and M. Tech. degree in control system from Kerala University, India in 1995 and 2000, respectively. She worked as an assistant professor at Department of Electrical and Electronic Engineering, Government Engineering College Thrissur, India from 2001 to 2013. Presently she is a Ph. D. degree candidate in electrical and electronics engineering at National Institute of Technology Tiruchirappalli, India.

Her research interests include nonlinear control, sliding mode control and optimization techniques.

E-mail: sunilasafa@gmail.com (Corresponding author)

ORCID iD: 0000-0002-9957-0235

V. Sankaranarayanan received the Ph. D. degree in systems and control engineering from Indian Institute of Technology Bombay, India in 2006, and served as a post-doctoral researcher at Istanbul Technical University, Turkey from 2006 to 2008. Currently, he is working as an associate professor at Department of Electrical and Electronics Engineering, National Institute of Technology, India.

His research interests include nonlinear control, control of underactuated systems, sliding mode control and constrained stabilization.

E-mail: sankariitb@gmail.com

K. Sundareswaran received the B. Tech. degree in electrical and electronics engineering and the M. Tech. degree in power electronics from the University of Calicut, India in 1988 and 1991, respectively, and received the Ph. D. degree in electrical engineering from Bharathidasan University, India in 2001. From 2005 to 2006, he was a professor with Department of Electrical Engineering, National Institute of Technology, India. He is currently a professor with Department of Electrical and Electronics Engineering, National Institute of Technology, India.

His research interests include power electronics, renewable energy systems and biologically inspired optimization techniques.

E-mail: kse@nitt.edu